Eur. Phys. J. Plus (2020) 135:733
https://doi.org/10.1140/epjp/s13360-020-00758-1

THE EUROPEAN PHYSICAL JOURNAL PLUS

Regular Article

The quaternionic Goos–Hänchen shift

Stefano De Leo[1,a], **Gisele Ducati**[2,b]

[1] Department of Applied Mathematics, State of University of Campinas, Campinas, Brazil
[2] Center of Mathematics, Computation and Cognition, Federal University of ABC, Santo André, Brazil

Received: 21 February 2020 / Accepted: 5 September 2020

Abstract We investigate the lateral displacement of electronic waves when partially and totally reflected by a quaternionic potential. Following the analogy between Quantum Mechanics and Optics, we introduce a refractive index for the complex and the pure quaternionic case. For incidence greater than the critical one (total reflection), the quaternionic potentials amplify the lateral displacement found in the complex case. For incidence below the critical angle, we find, in the quaternionic case, an additional shift. The analytical formula found for the quaternionic lateral displacement gives the possibility to observe quantitative and qualitative differences between the complex and quaternionic Goos–Hänchen shift.

1 Introduction

The Goos–Hänchen effect [1–3] is a well-known optical phenomenon regarding the lateral displacement that an optical beam of a finite cross section undergoes when it is totally reflected. In recent years, interesting applications are found in different areas like slow light processes [4,5], nanophotonics [6–8], photonic crystals [9–11], and seismic waves [12]. Experimental evidences of lateral displacement, angular deviations, and oscillatory phenomena due to the Goos–Hänchen shift are reported in [13–15]. For theoretical detailed reviews, we refer the reader to the tutorials given in refs. [16,17].

Quantitative and qualitative differences between complex and quaternionic Quantum Mechanics [18] had always been the main subject matter of many papers [19–34]. Such investigations surely contribute to motivate the worldwide community interested in the study of quaternionic formulation of Classical and Quantum Theories. In particular, a recent study on the analogy between quaternionic Quantum Mechanics and Optics [35] led to a quaternionic formulation of the Snell law. As it happens in the complex case, where, for total reflection, an additional phase appears in the reflection coefficient and generates the Goos–Hänchen shift, also for the quaternionic case additional phases appear in the reflection coefficient and create lateral displacements.

The paper is structured as follows: Sect. 2 presents the analogy between Quantum Mechanics and Optics, and it is important to understand the complex Goos–Hänchen shift. Since quaternionic Optics is not a known topic and the introduction of the quaternionic Snell law is short and pretty simple, for the convenience of the reader, in Sect. 3, we repeat the derivation

[a] e-mail: deleo@ime.unicamp.br (corresponding author)
[b] e-mail: ducati@ufabc.edu.br

Published online: 15 September 2020

of the quaternionic Snell law, thus making our exposition self-contained. In Sect. 4, we obtain the quaternionic reflection coefficient. The study of the additional phases for the complex and the pure quaternionic case is carried out in Sect. 5. The last section contains our final considerations and suggestions of possible future investigations.

2 Analogy between Optics and Quantum Mechanics

The analogy between Optics and Quantum Mechanics [36] allows to obtain the Snell law by analyzing the reflected and refracted waves for the planar (y, z) motion of a quantum mechanical particle in the presence of a stratified potential,

$$V(z) = \left\{ 0 \quad \text{for } z < 0 \quad \text{and} \quad V_1 \quad \text{for } z > 0 \right\}, \tag{1}$$

whose discontinuity is for convenience of calculation fixed at $z = 0$. The solution of the complex Schrödinger equation for $z < 0$ (region I) contains two waves, the incoming and the reflected ones, see Fig. 1,

$$\psi_{\rm I}(y, z) = \exp[\, i\, (p_y\, y + p_z\, z)/\hbar\,] + r\, \exp[\, i\, (p_y\, y - p_z\, z)/\hbar\,], \tag{2}$$

where r is the reflection coefficient. For $z > 0$ (region II), the solution contains the transmitted wave, see Fig. 1,

$$\psi_{\rm II}(y, z) = t\, \exp[\, i\, (p_y\, y + q_z\, z)/\hbar\,], \tag{3}$$

where t is the transmission coefficient. Note that due to the fact that the discontinuity is along the z-axis, the momentum component perpendicular to this axis is not changed when crossing the interface.

The reflection and transmission coefficients can then be obtained by imposing the continuity constraints to the wave function and its derivative. This yields to [36]

$$r = \frac{p_z - q_z}{p_z + q_z} \quad \text{and} \quad t = \frac{2\, p_z}{p_z + q_z}. \tag{4}$$

Region I represents the plane zone which is potential free. Consequently, from the Schrödinger equation,

$$E\, \psi_{\rm I}(y, z) = -\left[\frac{\hbar^2}{2\, m} \left(\partial_{yy} + \partial_{zz} \right) \right] \psi_{\rm I}(y, z), \tag{5}$$

we then obtain the well-known momentum/energy relation,

$$p_y^2 + p_z^2 = p^2 = 2\, m\, E.$$

In region II, the presence of a potential, V_1, implies

$$E\, \psi_{\rm II}(y, z) = -\left[\frac{\hbar^2}{2\, m} \left(\partial_{yy} + \partial_{zz} \right) - V_1 \right] \psi_{\rm II}(y, z), \tag{6}$$

from which we obtain the following momentum/energy relation

$$p_y^2 + q_z^2 = 2\, m\, (E - V_1) = \left(1 - \frac{V_1}{E} \right) p^2 = n^2 p^2, \tag{7}$$

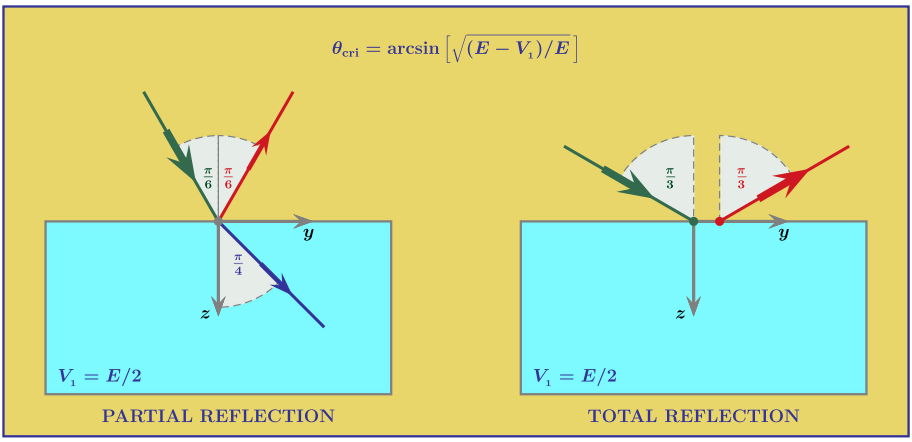

Fig. 1 Complex Goos–Hänchen shift. For the electronic reflected wave, a lateral displacement is found for incidence angles greater than the critical one (total reflection). For incoming particles with energy E equal to $2\,V_1$, the critical angle is $\pi/4$

where we have introduced the dimensionless quantity

$$n = \sqrt{1 - \frac{V_1}{E}}, \tag{8}$$

playing the role of the refractive index of Optics [37,38]. Observing that $p_z = p\,\cos\theta$ and $q_z = n\,p\,\cos\varphi$, see Fig. 1, from Eq.(7) we find

$$p^2\,\sin^2\theta + n^2 p^2\,\cos\varphi^2 = n^2 p^2,$$

and consequently, we recover, for a quantum non-relativistic particle crossing the interface between the free and the potential region, the well-known Snell law,

$$\sin\theta = n\,\sin\varphi. \tag{9}$$

2.1 The Goos–Hänchen shift

The Goos–Hänchen effect occurs when incident angles are bigger than the critical angle,

$$\theta_{\rm cri} \;=\; \arcsin[\,n\,] \;=\; \arcsin\left[\,\sqrt{\frac{E\;-\;V_1}{E}}\,\right]. \tag{10}$$

In order to calculate the lateral displacement, it is useful to rewrite the reflection coefficient in terms of the incident angle θ,

$$r = \frac{\cos\theta - n\,\cos\varphi}{\cos\theta + n\,\cos\varphi} = \frac{\cos\theta - \sqrt{n^2 - \sin^2\theta}}{\cos\theta + \sqrt{n^2 - \sin^2\theta}}. \tag{11}$$

For incidence angle satisfying the constraint $\sin\theta > n$, the reflection coefficient becomes

$$r = \exp\left[\,-2\,i\,\psi_{\rm GH}\,\right], \tag{12}$$

where

$$\psi_{\rm GH} = \arctan\left[\frac{\sqrt{\sin^2\theta - n^2}}{\cos\theta}\right] \tag{13}$$

is the phase, utilized by Artmann [2] to explain the Goos–Hänchen shift obtained for Transverse Electric waves [1]. Let us briefly recall why the presence of such a phase in the reflection coefficient implies a lateral displacement of the reflected particle. Let us first consider the incoming particle whose phase is given by

$$\phi_{\rm INC} = (p_y\, y_{\rm INC} + p_z\, z)/\hbar = p\,\left(\sin\theta\, y_{\rm INC} + \cos\theta\, z\right)/\hbar. \tag{14}$$

For wave packet, the main contribution to the motion of the particle comes from the minimum of such a phase [39]. By imposing a null derivative, we find

$$\frac{\partial\phi_{\rm INC}}{\partial\theta} = 0 \quad \Rightarrow \quad y_{\rm INC} = \tan\theta\, z. \tag{15}$$

For the reflected wave, when we are in the case of total reflection, the phase is given by

$$\phi_{\rm REF} = (p_y\, y_{\rm INC} - p_z\, z)/\hbar - 2\,\psi_{\rm GH} = p\,\left(\sin\theta\, y_{\rm REF} - \cos\theta\, z\right)/\hbar - 2\,\psi_{\rm GH}. \tag{16}$$

Consequently, we find

$$\frac{\partial\phi_{\rm REF}}{\partial\theta} = 0 \quad \Rightarrow \quad y_{\rm INC} = -\tan\theta\, z + \frac{2\,\hbar}{p\,\cos\theta}\frac{\partial\psi_{\rm GH}}{\partial\theta}. \tag{17}$$

Thus, the beam is reflected with an angle equal to the incident one (reflection law) but is laterally displaced. This lateral displacement, known as Goos–Hänchen shift, is given by

$$y_{\rm GH} = \frac{2\,\hbar}{p\,\cos\theta}\frac{\partial\psi_{\rm GH}}{\partial\theta} = \frac{2\,\hbar\,\tan\theta}{p\,\sqrt{\sin^2\theta - n^2}}. \tag{18}$$

In Fig. 1, we illustrate this phenomenon for a potential $V_1 = E/2$. In this case, the critical angle is $\pi/4$. We conclude this section by observing that the infinity for critical incidence is removed by using integral Fourier transforms [40–42].

3 The quaternionic Snell law

In the previous section, we have obtained the Snell law and the reflection coefficient for planar motion in the presence of complex potentials. In this section, we show how the Snell law is modified when we use a quaternionic potential in the Schrödinger equation. The time-independent Schrödinger equation in the presence of a quaternionic potential,

$$\boldsymbol{h}\cdot\boldsymbol{V}(z) = \left\{0 \quad \text{for } z<0 \quad \text{and} \quad i\,V_1 + j\,V_2 + k\,V_3 \quad \text{for } z>0\right\},$$

is given by [18]

$$E\,\Psi_{\rm II}(y,z)\,i = \left[-i\,\frac{\hbar^2}{2\,m}\left(\partial_{yy}+\partial_{zz}\right) + \boldsymbol{h}\cdot\boldsymbol{V}\right]\Psi_{\rm II}(y,z) = A_{\rm H}\,\Psi_{\rm II}(y,z). \tag{19}$$

Multiplying the previous equation from the left by the quaternionic anti-hermitian operator $A_{\rm H}$, we get

$$E^2\,\Psi_{\rm II}(y,z) = -\,A_{\rm H}^2\;\Psi_{\rm II}(y,z)$$
$$= \left[\frac{\hbar^4}{4\,m^2}\left(\partial_{yy}+\partial_{zz}\right)^2 - \frac{\hbar^2}{m}\,V_1\,\left(\partial_{yy}+\partial_{zz}\right) + |V|^2\right]\Psi_{\rm II}(y,z).$$

This equation allows to obtain the momentum solution which represents the quaternionic counterpart of q_z, i.e.,

$$p_y^2 + Q_z^2 = 2\,m\left(\sqrt{E^2 - V_2^2 - V_3^2} - V_1\right), \tag{20}$$

which characterizes the plane wave in the potential region,

$$\exp[\,i\,(\,p_y\,y + Q_z\,z)\,/\hbar\,],$$

and the additional solution

$$p_y^2 + \widetilde{Q}_z^2 = -\,2\,m\left(\sqrt{E^2 - V_2^2 - V_3^2} + V_1\right) \tag{21}$$

which generates *evanescent* wave solutions,

$$\exp[(i\,p_y\,y - |\widetilde{Q}_z|\,z)\,/\hbar].$$

Before giving the explicit quaternionic solutions for the reflection coefficient and comparing them with the complex case, let us now examine how the Snell law is modified by the *new* momentum Q_z. From Eq. (20), we find

$$p_y^2 + Q_z^2 = \left(\sqrt{1 - \frac{V_2^2+V_3^2}{E^2}} - \frac{V_1}{E}\right) 2\,m\,E = N^2\,p^2. \tag{22}$$

The presence of a quaternionic part in our potential generates the refractive index

$$N = \sqrt{\sqrt{1 - \frac{V_2^2+V_3^2}{E^2}} - \frac{V_1}{E}} \tag{23}$$

and consequently the *new* Snell law

$$\sin\theta = N\,\sin\phi. \tag{24}$$

4 The reflection amplitudes for quaternionic potentials

To obtain the reflection amplitude, we have to impose the continuity of the wave function and its derivative at the potential discontinuity $z = 0$. The quaternionic plane wave solutions are given by [19–24]

$$\Psi_{\rm I}(y,z) = \left\{\exp[i\,p_z z] + R\,\exp[-\,i\,p_z z] + j\,\widetilde{R}\,\exp[p_z z]\right\}\exp[i\,p_y y] \tag{25}$$

in the free potential region ($z < 0$) and

$$\Psi_{\rm II}(y,z) = \left\{(1+j\,\beta)\,T\,\exp[\,i\,Q_z z] + (\alpha + j\,)\,\widetilde{T}\,\exp[-|\widetilde{Q}_z|\,z]\right\}\exp[i\,p_y y], \tag{26}$$

where

$$\alpha = i\,\frac{(V_2 + i\,V_3)/E}{1+N^2}\,, \qquad \beta = -\,i\,\frac{(V_2 - i\,V_3)/E}{1+N^2},$$

in the potential region ($z > 0$). From the continuity equations of the pure quaternionic wave functions and their derivative, we get

$$\widetilde{R} = \beta\, T + \widetilde{T} \qquad \text{and} \qquad p_z\, \widetilde{R} = i\, \beta\, T\, Q_z - \widetilde{T}\, |\widetilde{Q}_z|, \tag{27}$$

from which we obtain

$$\widetilde{T} = \frac{i\, Q_z - p_z}{|\widetilde{Q}_z| + p_z}\, \beta\, T.$$

From the continuity equations of the complex wave functions and their derivative, we get

$$1 + R = T + \alpha\, \widetilde{T} \qquad \text{and} \qquad 1 - R = \frac{Q_z}{p_z}\, T + i\, \frac{|\widetilde{Q}_z|}{p_z}\, \alpha\, \widetilde{T}, \tag{28}$$

from which we obtain

$$\frac{1+R}{1-R} = \frac{p_z + \alpha\, p_z \widetilde{T}/T}{Q_z + i\, \alpha\, |\widetilde{Q}_z|\, \widetilde{T}/T}.$$

Finally,

$$R = \frac{(\,p_z\, -\, Q_z\,)(\,|\widetilde{Q}_z|\, +\, p_z\,)\, +\, \alpha\, \beta\, (\,i\, Q_z\, -\, p_z)(\,p_z\, -\, i\, |\widetilde{Q}_z|\,)}{(\,p_z\, +\, Q_z)(\,|\widetilde{Q}_z|\, +\, p_z\,)\, +\, \alpha\, \beta\, (\,i\, Q_z\, -\, p_z)(\,p_z\, +\, i\, |\widetilde{Q}_z|\,)}\,. \tag{29}$$

5 The quaternionic Goos–Hänchen shift

In this section, we study the Goos–Hänchen shift in the presence of a pure quaternionic potential. To compare the quaternionic shift with the standard complex one, we shall use the same refractive index for the pure quaternionic and complex potentials, i.e.,

$$n^2 \,=\, 1 \,-\, \frac{V_1}{E} \,=\, \sqrt{1 - \frac{V_2^2 \,+\, V_3^2}{E^2}}\,. \tag{30}$$

This means that, for example, a complex potential with $V_1 = E/2$ and a pure quaternionic potential with $\sqrt{V^2 + V_3^2} = \sqrt{3}\, E/2$ generates the same critical angle, $\theta_{\rm cri} = \pi/4$, see Fig. 2.

Observing that, for a pure quaternionic potential,

$$\alpha\, \beta \,=\, \frac{1 \,-\, n^2}{1 \,+\, n^2},$$

the reflection coefficient of Eq. (29) can be rewritten as follows

$$R \,=\, \frac{(\,1 \,+\, n^2\,)\,(\,p_z \,-\, Q_z\,)\,(\,|\widetilde{Q}_z|\, +\, p_z\,) \,+\, (\,1 \,-\, n^2\,)\,(\,i\, Q_z \,-\, p_z\,)\,(\,p_z \,-\, i\, |\widetilde{Q}_z|\,)}{(\,1 \,+\, n^2\,)\,(\,p_z \,+\, Q_z\,)\,(\,|\widetilde{Q}_z|\, +\, p_z\,) \,+\, (\,1 \,-\, n^2\,)\,(\,i\, Q_z \,-\, p_z\,)\,(\,p_z \,+\, i\, |\widetilde{Q}_z|\,)}. \tag{31}$$

where

$$\left\{\, p_z\,,\; Q_z\,,\; |\widetilde{Q}_z|\,\right\} \,=\, p\, \left\{ \cos\theta\,,\, \sqrt{n^2 \,-\, \sin^2\theta}\,,\, \sqrt{n^2 \,+\, \sin^2\theta} \right\}.$$

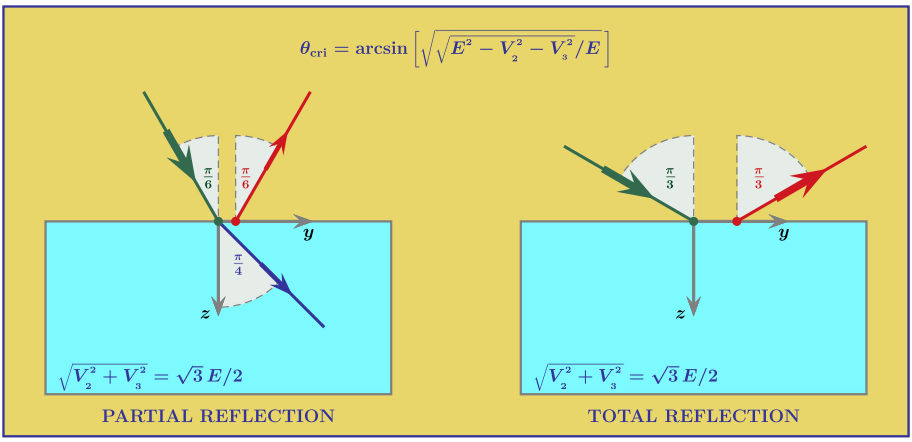

Fig. 2 Quaternionic Goos–Hänchen shift. In the case of a pure quaternionic potential and an incoming electronic wave with energy E equal to $2\sqrt{\left(V_2^2 + V_3^2\right)/3}$ the critical angle is $\pi/4$, as the complex case of Fig. 1. For pure quaternionic potential, a lateral displacement is also seen for incidence angles below the critical one

The reflection coefficients for complex and pure quaternionic potentials generating the same refractive index are plotted in Fig. 3, for refractive indexes corresponding to critical angles of $\pi/6$ (a), $\pi/4$ (b), and $\pi/3$ (c). or $\sin\theta > n$, we have

$$Q_z = i\,|Q_z| = i\,p\sqrt{\sin^2\theta - n^2}$$

and Eq. (31) becomes

$$R_{>} = \frac{(1+n^2)(p_z - i|Q_z|)(|\widetilde{Q}_z| + p_z) - (1-n^2)(p_z + |Q_z|)(p_z - i|\widetilde{Q}_z|)}{(1+n^2)(p_z + i|Q_z|)(|\widetilde{Q}_z| + p_z) - (1-n^2)(p_z + |Q_z|)(p_z + i|\widetilde{Q}_z|)}. \tag{32}$$

As happens for the complex case, the particle is totally reflected, see Fig. 3, and the reflection coefficient can be written in the following form

$$R_{>} = \exp[-2\,i\,\Psi_{GH}] \tag{33}$$

where

$$\tan\Psi_{GH} = \frac{(1+N^2)|Q_z|\,(p_z + |\widetilde{Q}_z|) - (1-N^2)|\widetilde{Q}_z|\,(p_z + |Q_z|)}{(1+N^2)\,p_z\,(p_z + |\widetilde{Q}_z|) - (1-N^2)\,p_z\,(p_z + |Q_z|)} \tag{34}$$

The stationary phase method yields

$$y_{GH}^{[quat]} = \frac{2\hbar}{p\cos\theta}\frac{\partial\Psi_{GH}}{\partial\theta}. \tag{35}$$

In Fig. 4, the adimensional Goos–Hänchen shift $p\,y_{GH}/\hbar$ is plotted for complex and pure quaternionic potentials. The quantitative differences appear for incidence angles greater than the critical one.

Qualitative differences appear for incidence below the critical angle, i.e., $\sin\theta < n$. In this case, differently of what happens for the complex case where the reflection coefficient

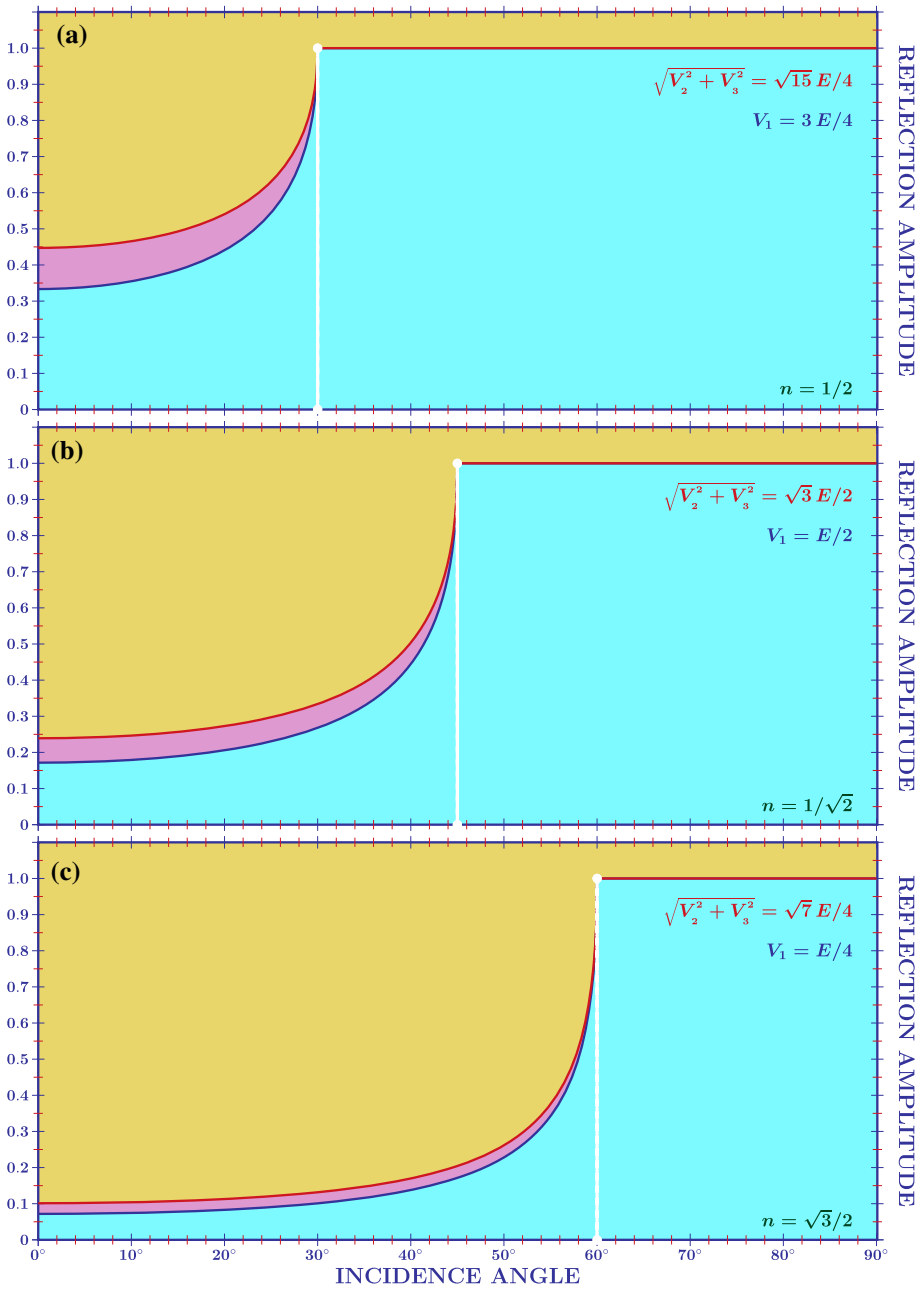

Fig. 3 Reflection amplitudes. The complex (blue line), $|r|$, and quaternionic (red line), $|R|$, reflection amplitudes are plotted as functions of the incident angle for different potentials chosen in order to obtain the same critical angle for the complex and quaternionic case. In **a**, the critical angle is $\pi/6$, in **b** $\pi/4$, and in **c** $\pi/3$

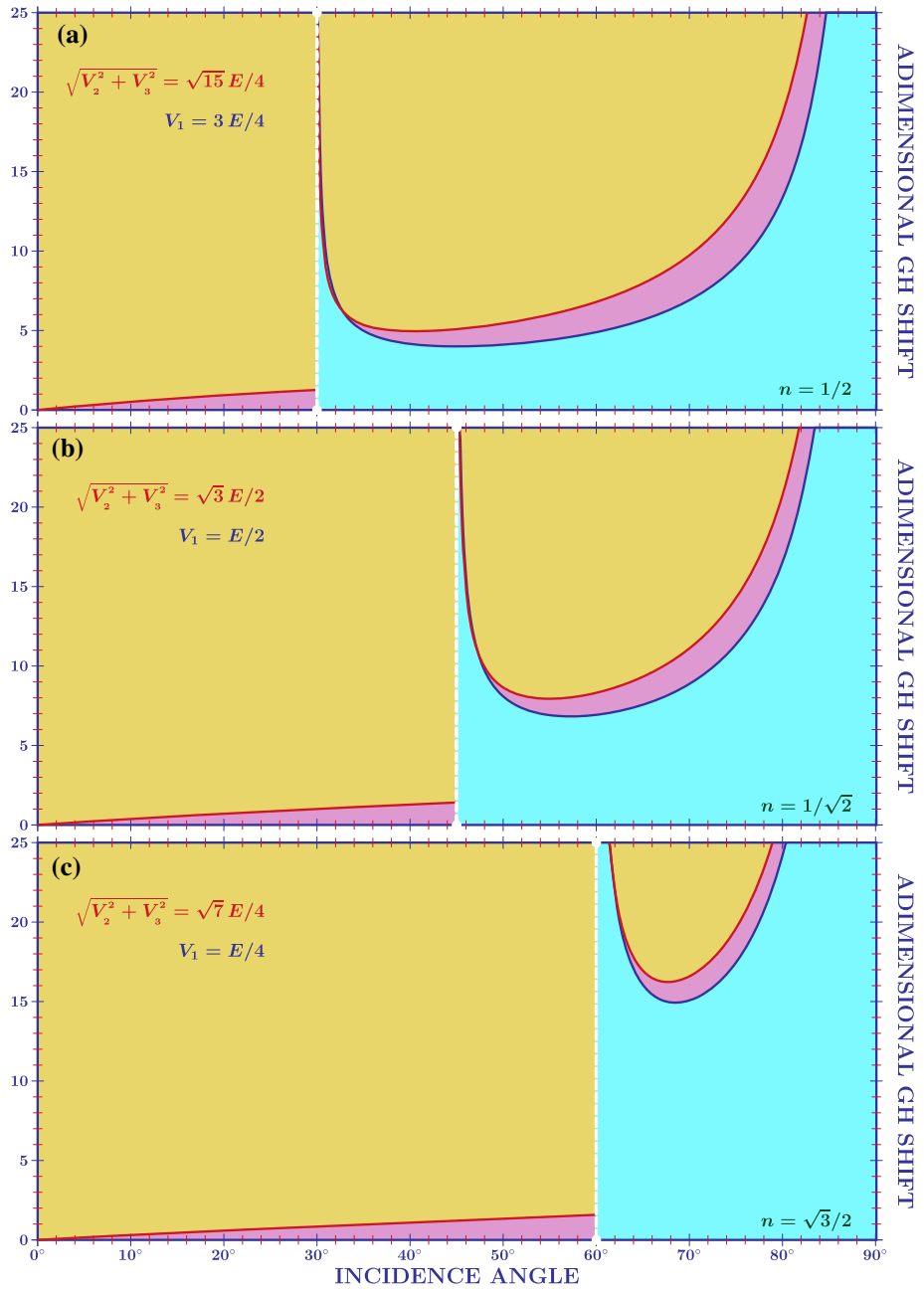

Fig. 4 Goos–Hänchen shifts. The adimensional lateral displacement, $p\, y_{\mathrm{GH}} / \hbar$, is plotted for complex (blue line) and pure quaternionic (red line) potentials generating the same critical angle. Quaternionic potential amplifies the effect for incidence greater than the critical one (total reflection). A new additional shift is seen for quaternionic potentials for incidence below the critical one

is real, the reflection coefficient is still a complex number,

$$R_{<} = \left| R_{<} \right| \exp[\, i\, (\, \Phi_{\mathrm{GH}}^{(\mathrm{num})} - \Phi_{\mathrm{GH}}^{(\mathrm{den})}\,], \tag{36}$$

with

$$\tan\left[\, \Phi_{\mathrm{GH}}^{(\mathrm{num})}\, \right] = \frac{(\,1 - n^2\,)\,(\,Q_z + |\,\widetilde{Q}_z|\,)\,p_z}{(\,1 + n^2\,)\,(\,p_z - Q_z\,)\,(\,|\widetilde{Q}_z| + p_z\,) - (\,1 - n^2\,)\,(\,p_z^2 - Q_z\,|\widetilde{Q}_z|\,)} \tag{37}$$

and

$$\tan\left[\, \Phi_{\mathrm{GH}}^{(\mathrm{den})}\, \right] = \frac{(\,1 - n^2\,)\,(\,Q_z - |\,\widetilde{Q}_z|\,)\,p_z}{(\,1 + n^2\,)\,(\,p_z + Q_z\,)\,(\,|\widetilde{Q}_z| + p_z\,) - (\,1 - n^2\,)\,(\,p_z^2 + Q_z\,|\widetilde{Q}_z|\,)}. \tag{38}$$

In the pure quaternionic case, a lateral displacement is thus present also for incidence below the critical angle,

$$\widetilde{y}_{\mathrm{GH}}^{[\mathrm{quat}]} = \frac{\hbar}{p\,\cos\theta}\left[\, \frac{\partial \Phi_{\mathrm{GH}}^{(\mathrm{den})}}{\partial\,\theta} - \frac{\partial \Phi_{\mathrm{GH}}^{(\mathrm{den})}}{\partial\,\theta}\, \right]. \tag{39}$$

This additional Goos–Hänchen shift is shown in the plots of Fig. 4.

6 Conclusions

Quantum Mechanics works very well, and Field Theory complements the prediction of Quantum Mechanics in the case of creation and annihilation of particles. However, this does not mean that it is impossible, in principle, to observe deviations from the complex Quantum Mechanics. Adler was the first to write a book on quaternionic Quantum Mechanics [18] and, starting from this milestone work, many papers investigated the possibility to find quantitative and qualitative differences between the complex and the quaternionic formulation of Quantum Mechanics. The analogy between Optics and Quantum Mechanics allows to propose, for electronic waves, a well-known phenomenon in Optics known as Goos–Hänchen shift, i.e., the lateral displacement of light when it is totally reflected by the interface between two media with different refractive indexes (the first one greater than the second one). In this paper, we have compared the shift of electronic waves when reflected by complex and pure quaternionic potentials. The analysis was done for complex and quaternionic potential generating the same critical angles. Analytical expression was obtained for the lateral displacement of electronic wave in the presence of pure quaternionic potentials. In the quaternionic case, the shift for incidence angles greater than the critical one amplifies the effect found in the complex case and presents a new phenomenon for incidence below the critical angle. The study was done by using plane waves. A future proposed work could be the analysis of the phenomena presented in this paper by using wave number distribution. This is usually done in the complex case [40,41], and it is fundamental to remove the infinity at the critical incidence and the discontinuity between the left and right regions, see Fig. 4. In the left region should appear the phenomenon of angular deviations and in the right region the pure Goos–Hänchen shift [17]. The critical region should be characterized by the composite Goos–Hänchen shift [13,15,42].

In this paper, we have studied in detail the case of a pure quaternionic potential. The most general quaternionic potential contains an additional complex part reproducing the standard

predictions of complex Quantum Mechanics. The pure complex part leads to a lateral shift for incidence greater than the critical one and the real part is responsible for the absorption effect. In this case, the pure quaternionic part has to be treated as a perturbation with respect to the complex one.

The possibility to propose an experiment to confirm or rule out quaternionic formulation of Quantum Mechanics was one of the main interests in this field, see, for example, the first proposals of ref. [43,44] investigating the effect of non-commutative phases and the recent one using metamaterial [45]. The main contribution of this article was the lateral displacements caused by the pure quaternionic before the critical angle. This effect, as well as the standard Goos–Hänchen shift, is of the order of the wavelength of the incident field. The idea for a possible proposal in testing quaternionic theories comes for the strict analogy between Quantum Mechanics and Optics. The study presented in this article has an immediate counterpart in the lateral shift of Transverse Electric waves. Material with a pure quaternionic refractive index should reproduce the additional lateral shift before the critical angle. It is also interesting to observe that extending the study of pure quaternionic material to Transverse Magnetic waves, we could use the Weak Measurements interference technique [46] to amplify such lateral displacements. In this view, the present work represents a preliminary study to stimulate future investigations in Quantum Mechanics as well in Optics.

Acknowledgements The authors thank an anonymous referee for his comments and suggestions. In particular, the authors appreciated very much the observations of the referee which have stimulated the discussion presented at the end of the concluding section. One of the authors (SdL) acknowledges the financial support from the CNPq (Grant Number 2018/03911) and the Fapesp (Grant Number 2019/06382-9).

References

1. F. Goos, H. Hänchen, Ein neuer und fundamentaler Versuch zur Totalreflexion. Ann. Phys. **436**, 333–346 (1947)
2. K. Artmann, Berechnung der Seitenversetzung des totalreflektierten Strahles. Ann. Phys. **437**, 87–102 (1948)
3. F. Goos, H. Hänchen, Neumessung des Strahlwersetzungseffektes bei Totalreflexion. Ann. Phys. **440**, 251–252 (1949)
4. Y. Hirai, K. Matsunaga, Y. Neo, T. Matsumoto, Observation of Goos–Hänchen shift in plasmon-induced transparency. Appl. Phys. Lett. **112–6**, 051101 (2018)
5. A. Malik, Y. Chaung, M. Abbas, Giant negative and positive Goos–Hänchen shifts via Doppler broadening effect. Laser Phys. **29**, 075201-6 (2019)
6. R. Halir et al., Ultra-broadband nanophotonic beamsplitter using an anisotropic sub-wavelength metamaterial. Laser Photonic Rev. **10**, 1039–1046 (2016)
7. L. Lambrechts, V. Ginis, J. Danckaert, P. Tassin, Transformation optics for surface phenomena: engineering the Goos–Hänchen effect. Phys. Rev. B **95**, 035427-5 (2017)
8. M. Zoghi, Goos–Hänchen and Imbert–Fedorov shifts in a two-dimensional array of gold nanoparticles. J. Nanophot. **12**, 016021-9 (2018)
9. Y. Dadoenkova et al., Goos–Hänchen effect in light transmission through biperiodic photonic-magnonic crystals. Phys. Rev. A **96**, 043804–6 (2017)
10. X. Wu, Goos–Hänchen shifts in tilted uniaxial crystals. Opt. Commun. **416**, 181–184 (2018)
11. I.V. Soboleva, V.V. Moskalenko, A.A. Fedyanin, Giant Goos–Hänchen effect and fano resonance at photonic crystal surfaces. Phys. Rev. Lett. **108**, 123901 (2012)
12. S. De Leo, R. Kraus, Incidence angles maximizing the Goos–Haenchen shift in seismic data analysis. Pure Appl. Geophys. **175**, 2023–2044 (2018)
13. O.J.S. Santana, S.A. Carvalho, S. De Leo, L.E.E. de Araujo, Weak measurement of the composite Goos–Hänchen shift in the critical region. Opt. Lett. **41**, 3884–3887 (2016)
14. S.A. Carvalho, S. De Leo, J.O.A. Huguenin, M. Martino, L. Silva, Experimental evidence of laser power oscillations induced by the relative Fresnel (Goos–Hänchen) phase. Laser Phys. Lett. **16**, 065001–5 (2019)

15. O.J.S. Santana, L.E.E. de Araujo, Direct measurement of the composite Goos–Hänchen shift of an optical beam. Opt. Lett. **43**, 4037–4040 (2018)
16. K.Y. Bliokh, A. Aiello, Goos–Hänchen and Imbert–Fedorov beam shifts: an overview. J. Opt. **15**, 014001–16 (2013)
17. S. De Leo, G.G. Maia, Lateral shifts and angular deviations of Gaussian optical beams reflected by and transmitted through dielectric blocks: A tutorial review. J. Mod. Opt. **66**, 2142–2194 (2019)
18. S. Adler, *Quaternionic Quantum Mechanics and Quantum Fields* (Oxford University Press, Oxford, 1995)
19. S. De Leo, G. Ducati, Quaternionic differential operators. J. Math. Phys. **42**, 2236–2265 (2001)
20. S. De Leo, G. Ducati, C.C. Nishi, Quaternionic potentials in non-relativistic quantum mechanics. J. Phys. A **35**, 5411–5426 (2002)
21. S. De Leo, G. Ducati, Quaternionic bound states. J. Phys. A **38**, 3443–3454 (2005)
22. S. De Leo, G. Ducati, T. Madureira, Analytic plane wave solutions for the quaternionic potential step. J. Math. Phys. **47**, 082106-15 (2006)
23. S. De Leo, G. Ducati, Quaternionic diffusion by a potential step. J. Math. Phys. **47**, 102104-9 (2006)
24. S. De Leo, G. Ducati, Quaternionic wave packets. J. Math. Phys. **48**, 052111-10 (2007)
25. T. Jiang, L. Chen, An algebraic method for Schrödinger equations in quaternionic quantum mechanics. Comput. Phys. Commun. **178**, 795–799 (2008)
26. F. Masillo, G. Scolarici, S. Sozzo, Proper versus improper mixtures: toward a quaternionic quantum mechanics. Theor. Math. Phys. **160**, 1006–1013 (2009)
27. S. De Leo, G. Ducati, Delay time in quaternionic quantum mechanics. J. Math. Phys. **53**, 022102–8 (2012)
28. S. De Leo, S. Giardino, Dirac solutions for quaternionic potentials. J. Math. Phys. **55**, 022301–10 (2014)
29. T. Jiang, Z. Jianga, S. Ling, An algebraic method for quaternion and complex Least Squares coneigen-problem in quantum mechanics. Appl. Math. Comput. **249**, 222–228 (2014)
30. S. De Leo, G. Ducati, S. Giradino, Quaternionic Dirac scattering. J. Phys. Math. **6**, 1000130–6 (2015)
31. H. Sobhani, H. Hassanabadi, Scattering in quantum mechanics under quaternionic Dirac delta potential. Can. J. Phys. **94**, 262–266 (2016)
32. H. Hassanabadi, H. Sobhani, A. Banerjee, Relativistic scattering of fermions in quaternionic quantum mechanics. Eur. Phys. J. C **77**, 581–5 (2017)
33. J. Gantner, On the equivalence of complex and quaternionic quantum mechanics. Math. Found. **5**, 357–390 (2018)
34. S. De Leo, C.A.A. Almeida, G. Ducati, Quaternionic perturbation theory. Eur. Phys. J. Plus **134**, 113–125 (2019)
35. S. De Leo, G.C. Ducati, The Snell law for quaternionic potentials. J. Math. Phys. **54**, 122109 (2013)
36. C.C. Tannoudji, B. Diu, F. Laloe, *Quantum Mechanics* (Wiley, Paris, 1977)
37. B.E.A. Saleh, M.C. Teich, *Fundamentals of Photonics* (Wiley, New York, 2007)
38. M. Born, E. Wolf, *Principles of Optics* (Cambridge University Press, Cambridge, 1999)
39. S. Carvalho, S. De Leo, The use of the stationary phase method as a mathematical tool to determine the path of optical beams. Am. J. Phys. **83**, 249–255 (2015)
40. M. Araújo, S. Carvalho, S. De Leo, The frequency crossover for the Goos–Hänchen shift. J. Mod. Opt. **60**, 1772–1780 (2013)
41. M. Araújo, S. De Leo, G. Maia, Closed form expression for the Goos–Hänchen lateral displacement. Phys. Rev. A **93**, 023801–9 (2016)
42. M. Araújo, S. De Leo, G. Maia, Oscillatory behavior of light in the composite Goos–Hänchen shift. Phys. Rev. A **95**, 053836–9 (2017)
43. A. Peres, Proposed test for complex versus quaternion quantum theory. Phys. Rev. Lett. **42**, 683–686 (1979)
44. H. Kaiser, E. George, S. Werner, Neutron interferometric search for quaternions in quantum mechanics. Phys. Rev. A **42**, 2276–2279 (1984)
45. L.M. Procopio et al., Single-photon test of hyper-complex quantum theories using a metamaterial. Nat. Commun. **8**, 15044-9 (1984)
46. M. Araújo, S. De Leo, G. Maia, Optimizing weak measurements to detect angular deviations. Ann. Phys. **529**, 1600357-20 (2017)